Temperature increase effects on a double-pass cavity type II second-harmonic generation: a model for depleted Gaussian continuous waves

Mohammad Sabaeian,* Fatemeh Sedaghat Jalil-Abadi, Mostafa Mohammad Rezaee, Alireza Motazedian, and Mohammadreza Shahzadeh

Physics Department, Faculty of Science, Shahid Chamran University of Ahvaz, Ahvaz 61357-43135, Iran

*Corresponding author: sabaeian@scu.ac.ir

Received 10 September 2014; revised 18 December 2014; accepted 21 December 2014; posted 23 December 2014 (Doc. ID 222620); published 28 January 2015

In this work, the effect of temperature increase on the efficiency of a double-pass cavity type II second-harmonic generation (SHG) is investigated. To this end, a depleted wave model describing the continuous-wave SHG process with fundamental Gaussian waves was developed. First, six coupled equations were proposed to model a double-pass cavity to generate the second harmonic of a Gaussian fundamental wave in type II configuration. Then, the effect of temperature increase in the nonlinear crystal due to the optical absorption was modeled. To do this, a mismatched phase arising from changes in refractive indices was added to the coupled equations. Although the nondepleted assumption is usually used in such problems, a simultaneous solving of coupled equations with assumption of fundamental beam depletion was performed. The results were obtained by a homemade code written in Intel Fortran, and show how the efficiency of the SHG process decreases when the crystal is warmed up by 5, 10, and 15 K. Dramatic reductions in SHG efficiency were observed due to small changes in temperature. The results show excellent agreement with the experimental data [Opt. Commun. **173**, 311–314 (2000)].

OCIS codes: (140.6810) Thermal effects; (190.0190) Nonlinear optics.
http://dx.doi.org/10.1364/AO.54.000869

1. Introduction

The need for continuous-wave (CW) green sources is increasing in many fields such as spectroscopy [1], biomedicine [2,3], and material processing [3]. One of the common methods to generate green laser lights is to use nonlinear crystals in which the near-infrared output of a Nd doped crystal is doubled via a second-harmonic generation (SHG) process [4]. Since the interaction length in CW setups for conventional nonlinear crystals such as KTP is much longer than the crystal length, the energy exchange between the fundamental and second-harmonic waves (SHWs) remains raw, and therefore the SHG conversion efficiency is lower [3]. In order to overcome this problem, multiple-pass configurations are used, in which fundamental and harmonic waves pass the crystal length several times to complete the interaction [1,3–5].

KTP is an excellent nonlinear crystal with high nonlinear conversion efficiency, high damage threshold, and wide allowable angle [6,7] when it is used to convert 1064 to 532 nm [8]. KTP crystal has been realized as an attractive nonlinear crystal for frequency-conversion applications [9–11] specially for SHG purposes [10,11].

To model the type II phase-matching SHG, one may use the sum frequency formalism in which, for fundamental waves having the same frequencies but different polarization, two polarization components of the electric field coincide: orthogonal

1559-128X/15/040869-07$15.00/0

ordinary and extraordinary directions of the doubling crystal. The SHW is then generated with a polarization along the extraordinary direction [12].

Although considering the Gaussian nature of the fundamental laser beams can be influential on the results, in some works the plane-wave approximation was used for the sake of simplicity in the calculations [13]. Many investigations regarding SHG have been performed in single-pass systems [3,7], while multiple-pass configurations, which are of great interest because of their higher efficiency [4,5,14], have been less modeled, especially when Gaussian beams are used. On the other hand, the optical absorption of beams when passing through the crystal leads to crystal warming. This can disturb the phase matching for crystals which are critically phase matched. The crystal warming, in fact, changes the ordinary and extraordinary refractive indices, and therefore the phase-matching condition of $n^{e,\omega} + n^{o,\omega} = 2n^{e,2\omega}$ can no longer be fulfilled.

Kumar and co-workers [3,4] achieved >55% SHG efficiency in a CW, single-pass device to generate 532 nm using MgO:sPPLT crystal. They studied the single-, double-, and multi-crystal schemes, and achieved a beam quality of ~1.6 for a TEM_{00} mode profile [3]. The investigation of CW, single-pass SHG was also carried out by Kumar *et al.* using periodically poled nonlinear crystals of PPKTP and MgO:sPPLT [15]. They achieved a maximum second-harmonic power of 9.6 W with a single-pass efficiency of 32.7% for MgO:sPPLT and 6.2 W with efficiency of 20.8% for PPKTP. The beam quality of the SHG was found to be different for powers >20 W between the two crystals [15]. Samanta *et al.* investigated the SHG in a single-pass CW fiber-laser-based green source [16]. They provided 11 W of TEM_{00} green power at 532 nm. The use of Yb-fiber laser in MgO:sPPLT for CW SHG in a single-pass device was also studied by Kumar *et al.* [17]. They achieved 2.3 W of single-mode output power at 812 nm. Liu *et al.* achieved 22.5% conversion efficiency of stable CW green radiation, at the incident pump power of 16 W, in a diode laser array, end-pumped, frequency-doubled Nd:$GdVO_4$/KTP with an output beam quality factor of $M^2 = 1.55$ [18]. Sabaeian *et al.* studied the SHG in a single-pass cavity with KTP crystal with thermal effect consideration [7]. They coupled the heat equation with CW SHG for single-pass configuration. Second-harmonic generation cavities can be intracavity or extracavity. In the intracavity configuration, the gain medium and the nonlinear crystal are placed inside the same resonator which is adopted in [18], while in the extracavity configuration, the nonlinear crystal is placed outside the fundamental wave cavity. This configuration is employed in [3,4,15–17].

In this work, we first present a model to investigate the SHG process in a double-pass cavity type II configuration when Gaussian CWs are used. The absorption terms due to optical absorption of fundamental as well as the SHWs in the nonlinear crystal are retained [13]. Then, a mismatched phase term corresponding to some temperature changes is considered in the model, and the efficiency is inspected under these temperature changes. In our model, six coupled equations are considered and solved simultaneously: two forward and backward wave equations for fundamental wave with ordinary polarization, two forward and backward equations for fundamental wave with extraordinary polarization, and two forward and backward equations for SHWs with extraordinary polarization. Since the simultaneous solving of these coupled equations is not possible analytically, we developed a numerical code. To this end, a homemade code based on the finite difference method was written in FORTRAN and run using a commercial PC with 4 GB RAM and a core i5 CPU. To the best of our knowledge, there is no other work that simultaneously considers double-pass type II SHG with Gaussian waves and temperature effects as a phase mismatching, so the gathering of all such effects and presentation of a comprehensive model is reported for the first time.

2. Theory

The nonlinear wave equation for a monochromatic polarized field in a medium with $\chi^{(2)}$ is given by [12]

$$\nabla^2 E_n(\vec{r},t) - \frac{\varepsilon^l}{c^2}\cdot\frac{\partial^2 E(\vec{r},t)}{\partial t^2} = \frac{1}{\varepsilon_0 c^2}\frac{\partial^2 P_n^{\mathrm{NL}}(\vec{r},t)}{\partial t^2}, \quad (1)$$

where $E(\vec{r},t)$, $P^{\mathrm{NL}}(\vec{r},t)$, c, and ε^l are the electric field, nonlinear polarization, speed of light, and dielectric constant, respectively. The dielectric constant consists of a real and an imaginary part expressed as

$$\varepsilon^{(l)} = \varepsilon_r^{(l)} + i\varepsilon_{im}^{(l)}. \quad (2)$$

According to Boyd [12], the field and polarization are given by

$$\mathrm{E}_n(\vec{r},t) = E_n(\vec{r})e^{ik_n z - i\omega_n t} + \mathrm{c.c.}, \quad (3)$$

$$P_n^{\mathrm{NL}}(\vec{r},t) = P_n^{\mathrm{NL}}(\vec{r})e^{ik_n z - i\omega_n t} + \mathrm{c.c.}, \quad (4)$$

where c.c. is the complex conjugate, ω is the angular frequency, and $k = n\omega/c$ is the wave vector. As we are using Gaussian beams with azimuthal symmetry, we use only r and z coordinates in cylindrical coordinates and keep only $\nabla^2 = \nabla_r^2 + \nabla_z^2$. Therefore, the nonlinear wave equation becomes

$$\frac{dE_n(r,z)}{dz} - \frac{i}{2k_n}\nabla_r^2 E_n(r,z) + \frac{\gamma_n}{2}E_n(r,z) = \frac{i\omega_n}{2n\varepsilon_0 c}P_n^{Nl}(r,z), \quad (5)$$

where $\gamma_n = \varepsilon_{im}\omega/nc$ is the absorption coefficient and $\varepsilon_0 = 8.85 \times 10^{-12}$ $\mathrm{C^2/Nm^2}$ is the vacuum permittivity.

A set of coupled equations for forward waves are therefore written as

$$\frac{dE_1(r,z)}{dz} - \frac{ic}{2n_1\omega_1}\nabla_r^2 E_1(r,z) + \frac{\gamma_1}{2}E_1(r,z) = \frac{2i\omega_1}{n_1 c} d_{\text{eff}} E_2^*(r,z)E_3(r,z)e^{-i\Delta kz}, \quad (6)$$

$$\frac{dE_2(r,z)}{dz} - \frac{ic}{2n_2\omega_2}\nabla_r^2 E_2(r,z) + \frac{\gamma_2}{2}E_2(r,z) = \frac{2i\omega_2}{n_2 c} d_{\text{eff}} E_1^*(r,z)E_3(r,z)e^{-i\Delta kz}, \quad (7)$$

$$\frac{dE_3(r,z)}{dz} - \frac{ic}{2n_3\omega_3}\nabla_r^2 E_3(r,z) + \frac{\gamma_3}{2}E_3(r,z) = \frac{2i\omega_3}{n_3 c} d_{\text{eff}} E_1(r,z)E_2(r,z)e^{i\Delta kz}, \quad (8)$$

where $\Delta k = k_1 + k_2 - k_3$ is the vector mismatching and $d_{\text{eff}} = 2\chi^{(2)}$ is the effective nonlinear coefficient [12]. For a KTP crystal which is cut at $\theta = 24.77°$ and $\phi = 90°$ [7], the phase matching occurs at $T = 300$ K. In the type II SHG, the fundamental waves with equal frequencies of $\omega_1 = \omega_2 = \omega$ are irradiated onto the crystal with orthogonal polarizations, i.e., one along the ordinary and another along the extraordinary direction, and the phase-matching condition ($\Delta\vec{k} = \vec{k}_1 + \vec{k}_2 - \vec{k}_3 = 0$) would be fulfilled for the SHW with frequency of $\omega_3 = 2\omega$ along the extraordinary direction. The phase-matching condition is fulfilled if $n^{\omega,o}\omega + n^{\omega,e}\omega = n^{2\omega,e}2\omega$ [7]. In the previous equations, we used $n^{o,\omega} = n_1$, $n^{e,\omega} = n_2$, and $n^{e,2\omega} = n_3$. However, if the crystal temperature changes, a thermally induced phase mismatching [7] occurs and the phase matching would disturb. To calculate the thermally induced phase mismatching, $\Delta\varphi = \Delta kz$, we used the formulas presented in Ref. [7]. The relation of $\Delta k = [(2\pi/\lambda_1)n_1(T) + (2\pi/\lambda_2)n_2(T) - (2\pi/\lambda_3)n_3(T)]$ with $T = T_{\text{PM}} + \Delta T$, where T_{PM} is phase-matched temperature, $\lambda_1 = \lambda_2 = 1064$ nm, and $\lambda_3 = 532$ nm, is used to calculate the mismatched phase.

In order to solve Eqs. (6)–(8), we introduce change of variables, that is, we use dimensionless variables ψ' as the ratio of wave intensity to initial wave intensity at $z = 0$:

$$E^{o,\omega} = \sqrt{\frac{P_f}{2n^{o,\omega}c\varepsilon_0\pi\omega_f^2}}\psi_1(r,z), \quad (9)$$

$$E^{e,\omega} = \sqrt{\frac{P_f}{2n^{e,\omega}c\varepsilon_0\pi\omega_f^2}}\psi_2(r,z), \quad (10)$$

$$E^{e,2\omega} = \sqrt{\frac{P_f}{n^{e,2\omega}c\varepsilon_0\pi\omega_f^2}}\psi_3(r,z), \quad (11)$$

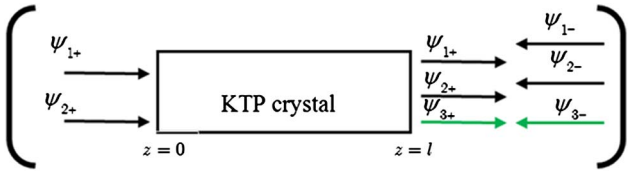

Fig. 1. Forward and backward waves in the double-pass cavity. $z = 0$ and $z = l$ are assumed at the beginning and end faces of the crystal, respectively.

in which P_f and ω_f describe the fundamental power and beam spot size, respectively. Accordingly, the quantity $\eta_i = |\psi_i|^2$ with $i = 1, 2, 3$ denotes the intensity efficiency for various waves.

Figure 1 shows a double-pass cavity scheme in which all fundamental and SHWs pass the crystal two times. A realistic configuration of double-pass cavity is shown in Fig. 2, which has been taken from Ref. [19]. In this scheme, the fundamental wave is generated in a Nd:YAG cavity composed of mirrors M_3 and M_1, Brewster plate, and aperture. A 1064 nm wave is then reflected by mirror M_1 and enters the nonlinear cavity composed of mirrors M_2 and M_1 and nonlinear crystal. This scheme constitutes an intracavity SHG configuration. According to Fig. 1, the backward waves are generated through reflection from mirrors and mathematically are modeled by letting $\vec{k} \to -\vec{k}$ in nonlinear Eqs. (6)–(8). After some mathematical treatments, the final dimensionless equations for forward and backward fundamental and SHWs read as

$$\pm\frac{d\psi_{1\pm}(r,z)}{dz} - \frac{ic}{2n^{o,\omega}\omega}\nabla_r^2\psi_{1\pm}(r,z) + \frac{\gamma_1}{2}\psi_{1\pm}(r,z) = \frac{i}{l\sqrt{n^{o,\omega}n^{e,\omega}n^{e,2\omega}}}\psi_{3\pm}(r,z)\psi_{2\pm}^*(r,z) \times \exp(\mp\Delta kz), \quad (12)$$

$$\pm\frac{d\psi_{2\pm}(r,z)}{dz} - \frac{ic}{2n^{e,\omega}\omega}\nabla_r^2\psi_{2\pm}(r,z) + \frac{\gamma_2}{2}\psi_{2\pm}(r,z) = \frac{i}{l\sqrt{n^{o,\omega}n^{e,\omega}n^{e,2\omega}}}\psi_{3\pm}(r,z)\psi_{1\pm}^*(r,z) \times \exp(\mp\Delta kz), \quad (13)$$

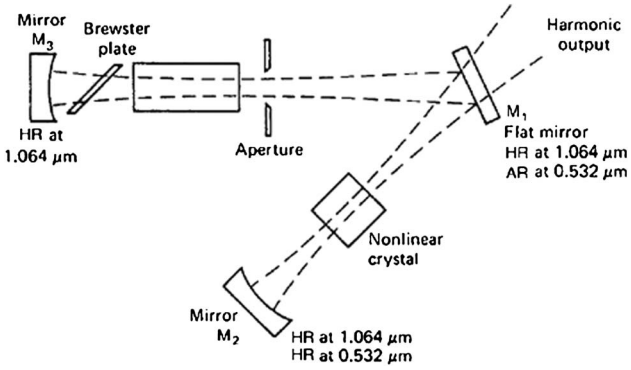

Fig. 2. Schematic configuration of an intracavity SHG [19]. The KTP crystal is placed between the M_2 and M_1 mirrors.

$$\pm\frac{d\psi_{3\pm}(r,z)}{dz}-\frac{ic}{4n^{e,2\omega}\omega}\nabla_r^2\psi_{3\pm}(r,z)+\frac{\gamma_3}{2}\psi_{3\pm}(r,z)$$
$$=\frac{i}{l\sqrt{n^{o,\omega}n^{e,\omega}n^{e,2\omega}}}\psi_{1\pm}(r,z)\psi_{2\pm}(r,z)\times\exp(\pm\Delta kz), \quad (14)$$

where the upper (lower) sign indicates the forward (backward) waves. The interaction length defined by $l=\sqrt{\varepsilon_0c^3\pi\omega_f^2/4\omega^2d_{\text{eff}}^2P_f}$ is an important parameter to determining the SHG efficiency. In fact, the interaction length determines a length over which a huge amount of nonlinear interaction is accomplished. As the formula shows, by increasing the fundamental beam power and/or decreasing the beam spot size, i.e., by increasing the fundamental beam intensity, the interaction length is shortened and the nonlinear interaction gets complete over a shorter distance.

To account for Gaussian fundamental beams, the boundary conditions of $\psi_{1+}(r,z=0)=\psi_{2+}(r,z=0)=\exp(-r^2/\omega_f^2)$ are used. For the SHW, the condition of $\psi_{3+}(r,z=0)=0$ is used at $z=0$. The forward and backward waves must satisfy the condition of $\psi_{i-}(r,z=L)=\sqrt{R_{if}}\psi_{i+}(r,z=L)$ with $i=1,2,3$, where R_{if} is the reflective power of front mirrors. $z=0$ and $z=l$ are assumed at the beginning and end faces of the nonlinear crystal, respectively. A realistic double-pass cavity SHG setup is shown in Fig. 2 [19].

3. Results

To solve coupled Eqs. (12)–(14), we adopted a finite difference method, wrote a code in FORTRAN, and ran it with the Linux operating system. The physical procedure of solving Eqs. (12)–(14) is as follows: first, the forward equations are solved by the numerical forward difference method. At the end of the cavity, the forward waves are refracted back and the backward waves are produced. This event is modeled by satisfying the condition of $\psi_{i-}(r,z=L)=\sqrt{R_{if}}\psi_{i+}(r,z=L)$. Then, with the numerical backward difference method, the backward waves are modeled. The results were obtained by the following parameters: the absorption coefficients of KTP at fundamental wavelength are $\gamma_1=\gamma_2=0.5\ \text{m}^{-1}$ and, for second-harmonic wavelength, is $\gamma_3=4\ \text{m}^{-1}$ [20]. The refractive indices are $n^{o,\omega}=n_1=1.8296$, $n^{e,\omega}=n_2=1.7466$, and $n^{e,2\omega}=n_3=1.7881$ [21]. The effective nonlinear coefficient is $d_{\text{eff}}=7.3$ pm/V[21]. The radius and length of the cylindrical crystal is 1.5 and 11 mm, respectively [18]. The reflectivity of the mirrors is $R_{1f}=R_{2f}=R_{3f}=0.99$; that is, for front mirrors, we used highly reflective mirrors. The meshing of crystal is of importance in obtaining accurate results. In this work, the best meshing is 300×200 for r and z coordinates for a beam spot size of 50 μm.

Figure 3 shows the *second-harmonic efficiency* for forward and backward beams at phase-matched temperature along the crystal length for the powers of 10, 30, and 80 W and beam spot size of 50 μm. According to this figure, the efficiency increases with power due to decrease in interaction length. Also, the second-harmonic efficiency for backward beams is much more than that of forward beams, proving the fact that the efficiency in double-pass configurations is greater than in single-pass ones.

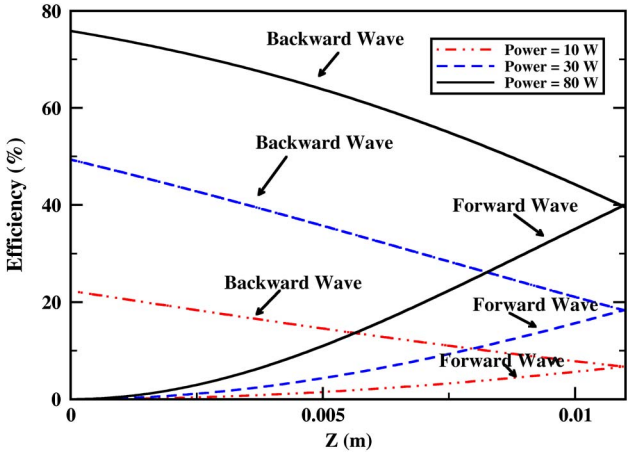

Fig. 3. Second-harmonic efficiency as a function of the crystal length for forward and backward beams for three powers of fundamental waves and beam spot size of 50 μm.

The efficiency of forward and backward *fundamental beams* along the crystal length for powers of 10, 30, and 80 W and beam spot size of 50 μm is plotted in Fig. 4. A faster drop in fundamental wave efficiency is seen for larger powers, indicating progress in energy transfer from the fundamental to the SHWs.

In Fig. 5, we examine the role of beam spot size. The second-harmonic efficiency of backward beams with respect to the power for four beam spot sizes of 30, 40, 50, and 60 μm is shown in Fig. 5, showing an increase in the efficiency with decrease in the beam spot size. This is due to decrease in the length of the interaction.

Figure 6 shows the second-harmonic efficiency as a function of crystal length. The powers are 10, 30, and 80 W, and the beam spot size of 50 μm has been chosen. As the figure shows, the second-harmonic efficiency increases with increase in the crystal length. It is safe to say that, for a CW SHG, due to the shortening of interaction length, longer crystals provide higher efficiencies. However, it should be noted that elongation of the crystal should be continued up to reaching the optimum efficiencies [22]. Unnecessary elongation without any contrivance leads to reduction in SHG efficiency due to optical absorption and converting back the energy of SHW toward the fundamental wave.

The results achieved so far have been calculated in the phase-matched temperature. To see the effect of temperature changes, we examined the influence of 5, 10, and 15 K temperature change in the crystal temperature. Figure 7 shows the SHG efficiency along the crystal length at the various temperatures.

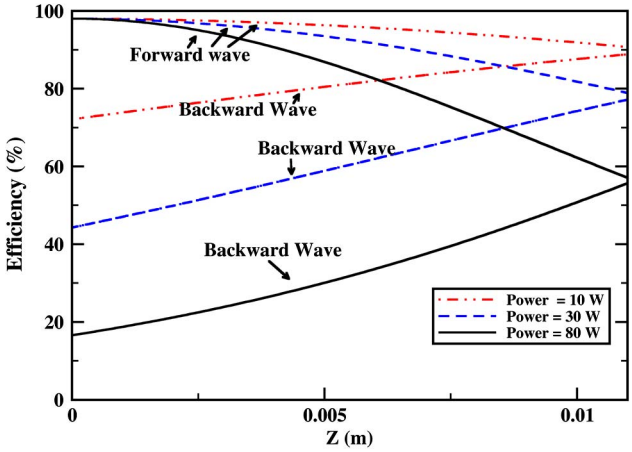

Fig. 4. Efficiency of fundamental beams as a function of the crystal length for forward and backward beams for three powers and beam spot size of 50 μm.

A spot size of $\omega_f = 50$ μm and pump power of $P_f = 60$ W have been used to draw the curves. Figure 7 clearly shows the reduction in SHG efficiency with small increase in temperature. In experimental setups, usually the crystal is placed in an oven and kept in a constant temperature. Nevertheless, the finiteness of thermal relaxation time of the crystal leads to some temperature increases, which are inevitable. Our results emphasize the critical role of temperature change and show that one should be cautious about even a little temperature increase in the crystal causing dramatic reductions in efficiency.

Figure 8 shows the SHG efficiency as a function of fundamental power at several temperature changes. As the figure shows, the efficiency in each case increases with increase in the fundamental power. The growing up of the efficiency with input power is a result of shortening the interaction length, indicating that in CW SHG, the interaction is larger than crystal length and is decreased with increase in both power and/or beam spot size. The curves in Fig. 8 have been calculated with this assumption that,

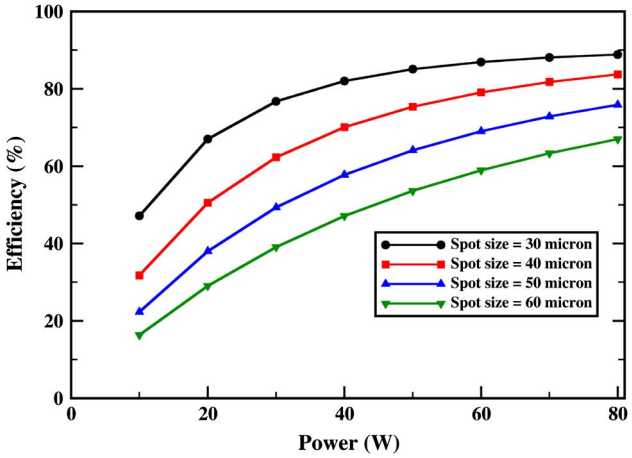

Fig. 5. Second-harmonic efficiency of backward beams with respect to power for four beam spot sizes.

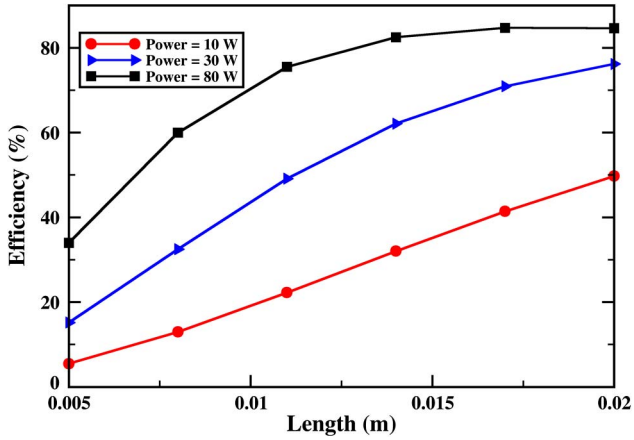

Fig. 6. Second-harmonic efficiency as a function of length of the crystal for three powers and 50 μm beam spot size.

for higher input fundamental powers, the crystal temperature does not change. This event, in practice, may be hard to reach since when the pump power is increased, the portion on converting pumping power to heat is increased. For $T = 315$ K, the efficiency is very low and cannot be grown even by increasing the power. Higher mismatched phase results in lower efficiency amplitude with more oscillations, which is not shown in the figure. The exponential term appearing in SHG formalism seems to be very influential in the amount of efficiency.

In order to compare our numerical results with those of experimental works, we adopted our parameters used according to Ref. [18]. The fundamental power of 10.1 W was used according to this work. Figure 9 shows the variations (in terms of efficiency) of the second-harmonic and fundamental waves along the crystal length. We calculated the SHG efficiency of 23%, which is in excellent agreement with the data obtained in Ref. [18]; they achieved an efficiency of 22.5%. It seems that, for 10.1 W pump

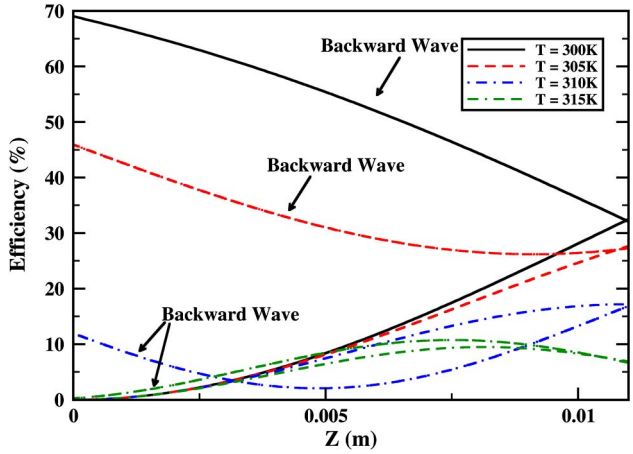

Fig. 7. Efficiency of SHG along the crystal length for phase-matched temperature (solid), 305 K (dashed), 310 K (dashed–dotted), and 315 K (dashed–dashed–dotted) curves. A beam spot size of $\omega_f = 50$ μm and fundamental power of $P_f = 60$ W have been considered. The unlabeled curves show forward beams.

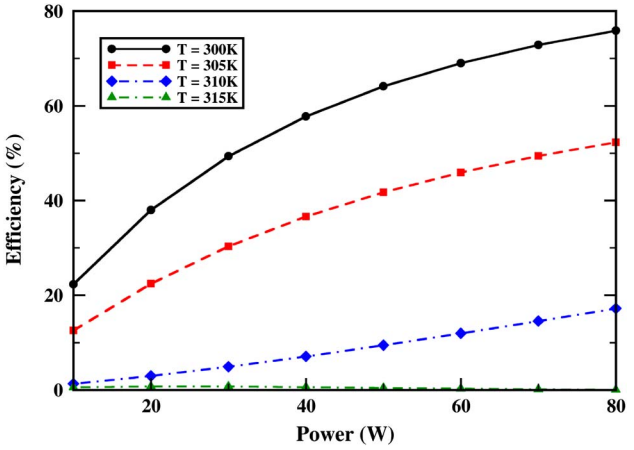

Fig. 8. SHG efficiency as a function of fundamental power for four crystal temperature increases.

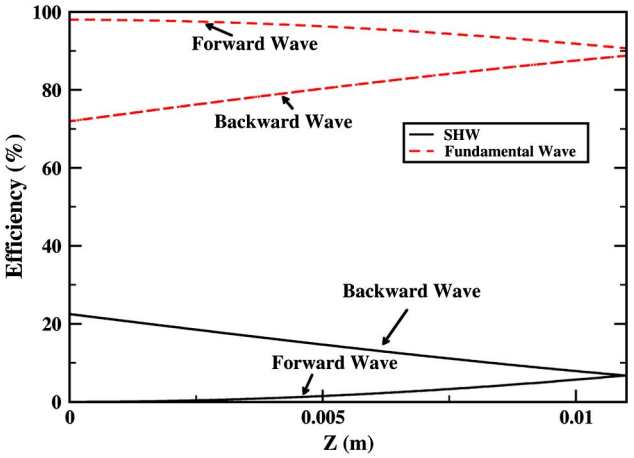

Fig. 9. Efficiency of the forward and backward fundamental and second-harmonic waves (SHWs) along the crystal length for the incident fundamental pump power of 10.1 W [18]. The efficiency of the SHG is 23%.

power, the thermal effects are moderate. It is worth noting that Liu *et al.*, by wrapping the crystal in indium foil and using an active cooler, compensated for the temperature increase in the nonlinear crystal.

In this work, we investigated SHG using Gaussian waves. Our inspection for plane waves shows that the results along the z axis and at $r = 0$ are the same. However, when Gaussian waves are considered for fundamental waves, the efficiencies drop quickly along the r direction, which is a property of Gaussian waves. The dropping rate depends on beam spot size.

4. Conclusion

In summary, double-pass type II SHG, which has been less modeled in the literature, was considered and a model based on a coupled set of six equations has been adopted to describe the efficiency of SHG. The model used CW Gaussian waves as fundamental waves and the resultant wave was also Gaussian SHWs. A numerical finite difference method has been adopted to solve the equations. The results, which have been compared with experimental data, show how the nonlinear interaction continues when the waves return back to the crystal, leading to a higher efficiency. Furthermore, the effects of temperature increase on the SHG efficiency as a mismatched phase was investigated. The results revealed that even a small temperature change in the crystal causes a dramatic reduction in the SHG efficiency.

The authors thank Shahid Chamran, University of Ahvaz, Iran, for supporting this work.

References

1. J. Bai and G. Chen, "Continuous-wave diode-laser end-pumped Nd:YVO_4/KTP high-power solid-state green laser," Opt. Laser Technol. **34**, 333–336 (2002).
2. M. Tsunekane, N. Taguchi, and H. Inaba, "Elimination of chaos in a multilongitudinal-mode, diode-pumped, 6-W continuous-wave, intracavity-doubled Nd:YAG laser," Opt. Lett. **22**, 1000–1002 (1997).
3. S. C. Kumar, G. Samanta, K. Devi, and M. Ebrahim-Zadeh, "High-efficiency, multicrystal, single-pass, continuous-wave second harmonic generation," Opt. Express **19**, 11152–11169 (2011).
4. G. Samanta, S. C. Kumar, K. Devi, and M. Ebrahim-Zadeh, "Multicrystal, continuous-wave, single-pass second-harmonic generation with 56% efficiency," Opt. Lett. **35**, 3513–3515 (2010).
5. K. Schneider, S. Schiller, J. Mlynek, M. Bode, and I. Freitag, "1.1-W single-frequency 532-nm radiation by second-harmonic generation of a miniature Nd:YAG ring laser," Opt. Lett. **21**, 1999–2001 (1996).
6. J. D. Bierlein and H. Vanherzeele, "Potassium titanyl phosphate: properties and new applications," J. Opt. Soc. Am. B **6**, 622–633 (1989).
7. M. Sabaeian, L. Mousave, and H. Nadgaran, "Investigation of thermally-induced phase mismatching in continuous-wave second harmonic generation: a theoretical model," Opt. Express **18**, 18732–18743 (2010).
8. J. Zheng, S. Zhao, Q. Wang, X. Zhang, and L. Chen, "Influence of thermal effect on KTP type-II phase-matching second-harmonic generation," Opt. Commun. **199**, 207–214 (2001).
9. T. Taira and T. Kobayashi, "Intracavity frequency doubling and Q switching in diode-laser-pumped Nd:YVO_4 lasers," Appl. Opt. **34**, 4298–4301 (1995).
10. G. Hansson, H. Karlsson, S. Wang, and F. Laurell, "Transmission measurements in KTP and isomorphic compounds," Appl. Opt. **39**, 5058–5069 (2000).
11. E. Rafailov, W. Sibbett, A. Mooradian, J. McInerney, H. Karlsson, S. Wang, and F. Laurell, "Efficient frequency doubling of a vertical-extended-cavity surface-emitting laser diode by use of a periodically poled KTP crystal," Opt. Lett. **28**, 2091–2093 (2003).
12. R. W. Boyd, *Nonlinear Optics* (Elsevier, 2008).
13. S. Spiekermann, F. Laurell, V. Pasiskevicius, H. Karlsson, and I. Freitag, "Optimizing non-resonant frequency conversion in periodically poled media," Appl. Phys. B **79**, 211–219 (2004).
14. G. Imeshev, M. Proctor, and M. Fejer, "Phase correction in double-pass quasi-phase-matched second-harmonic generation with a wedged crystal," Opt. Lett. **23**, 165–167 (1998).
15. S. C. Kumar, G. Samanta, and M. Ebrahim-Zadeh, "High-power, single-frequency, continuous-wave second-harmonic-generation of ytterbium fiber laser in PPKTP and MgO:sPPLT," Opt. Express **17**, 13711–13726 (2009).
16. G. Samanta, S. Chaitanya Kumar, K. Devi, and M. Ebrahim-Zadeh, "High-power, continuous-wave Ti:sapphire laser pumped by fiber-laser green source at 532 nm," Opt. Lasers Eng. **50**, 215–219 (2012).

17. S. C. Kumar, G. K. Samanta, K. Devi, S. Sanguinetti, and M. Ebrahim-Zadeh, "Single-frequency, high-power, continuous-wave fiber-laser-pumped Ti:sapphire laser," Appl. Opt. **51**, 15–20 (2012).
18. J. Liu, Z. Shao, H. Zhang, X. Meng, L. Zhu, J. Wang, Y. Liu, and M. Jiang, "Diode-laser-array end-pumped intracavity frequency-doubled 3.6 W CW Nd:$GdVO_4$/KTP green laser," Opt. Commun. **173**, 311–314 (2000).
19. W. Koechner and M. Bass, *Solid-State Lasers: A Graduate Text* (Springer, 2003).
20. D. Nikogosian, *Nonlinear Optical Crystals: A Complete Survey* (Springer, 2005).
21. K. Asaumi, "Second-harmonic power of $KTiOPO_4$ with double refraction," Appl. Phys. B **54**, 265–270 (1992).
22. M. Sabaeian, F. S. Jlil-Abadi, M. M. Rezaee, and A. Motazedian, "Heat coupled Gaussian continuous-wave double-pass type-II second harmonic generation: inclusion of thermally induced phase mismatching and thermal lensing," Opt. Express **22**, 25615–25628 (2014).